THE GROWTH OF THE MIXED LAYER IN A STRATIFIED FLUID DUE TO PENETRATIVE CONVECTION

F. D. HEIDT

Dornier System GmbH, 7990 Friedrichshafen, F.R.G.*

(Received 31 January, 1977)

Abstract. This paper describes a theoretical and experimental study of penetrative convection within an initially thermally stably stratified fluid heated from below. Emphasis is placed on the experimental investigation of the growth of the mixed layer and the entrainment at its boundary. Both processes play an important role in density-induced geophysical phenomena such as the lifting of an inversion layer during the morning and the deepening of a thermocline in a lake during the fall.

Many laboratory experiments with water as the experimental fluid were performed, in which the convection process was generated and visualised. The height of the mixed layer, heat transfer across the bottom interface and temperature profiles were measured as functions of time.

Theoretically-based analytical equations are given, which predict the thickness and temperature of the mixed layer. The equations involve one empirical factor characterising the entrainment rate at the interface between the mixed and the upper stable layer.

The experimental results confirm the theoretical equations and show that the empirical factor is a constant. From this, an entrainment rate is calculated which agrees well with values presented in the meteorological literature.

1. Introduction

An initially stagnant, linearly thermally stratified fluid with the temperature gradient γ = constant is heated from below (Figure 1). Above a critical Rayleigh number of the order of magnitude 1000, instabilities in the form of mushroom-like convective

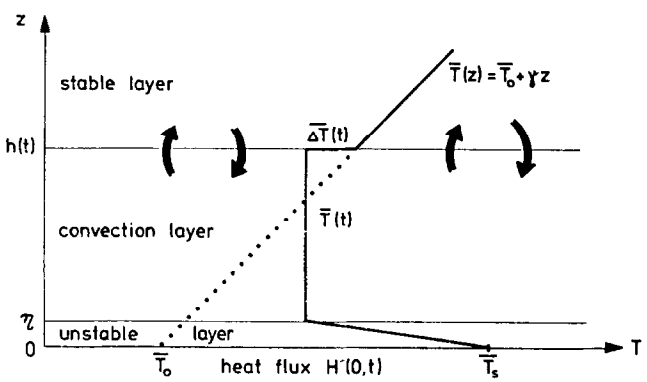

Fig. 1. Idealised three-layer model demonstrating the formation of temperature profiles in a stable stratification due to bottom heating. The height η of the unstable layer is independent of time. The temperature $\bar{T}(t)$ of the convection layer is independent of the height z. The temperature discontinuity $\Delta\bar{T}(t)$ between the stable and convection layers results in a heat flux in the z-direction.

* Work performed at Sonderforschungsbereich 80, University of Karlsruhe.

Boundary-Layer Meteorology **12** (1977) 439–461.

elements penetrate the overlying stable layer. The elements or thermals form a nearly homogeneous mixed layer of temperature $\bar{T}(t)$ and height $h(t)$, both of which increase with time.

The initially stably stratified fluid separates into three regions: a thin unstable layer of thickness η near the bottom, a mixed layer of height $h(t)$ and temperature $\bar{T}(t)$, and the stable layer above, which is bombarded and eroded from below by the thermals.

The entrainment process can be described using the following simple physical model. Within the mixed layer, the ascending thermals have nearly the same temperature $\bar{T}(t)$. The mass transport, produced by the thermals from the mixed layer into the stable layer, which has a temperature greater than $\bar{T}(t)$, must be balanced by an equal mass flux from the stable layer downward. At the height $h(t)$, this results in a net heat flux $H(h, t)$ which is directed downward.

In the atmosphere, a stable stratification is often observed at night. Sun irradiation warms the soil during the morning and creates a sensible heat flux which produces a mixed layer of several hundred to two thousand metres. (The temperature distribution is the same as the one described above if actual temperatures are replaced by potential temperatures.)

During the fall, the water surface of a stably stratified lake or reservoir is cooled mostly by radiation and evaporation. This generates negative buoyancy forces which initiate a penetrative convection process. The developing mixed layer is called the epilimnion and is separated from the underlying stable layer, the hypolimnion, by the thermocline. The corresponding fields of temperature and velocity are of great importance for the distribution of oxygen and nutrients within the lake. Some aspects of this problem are considered in the papers of Okubo (1953), Spangenberg and Rowland (1961), Foster (1965) and Farmer (1975).

The influence of surface heating on the height of the inversion layer was first discussed by Ball (1960) assuming $H(h, t) = -H(0, t)$. Lilly (1968) discussed the alternate assumptions $H(h, t) = 0$ and $H(h, t) = -H(0, t)$. Carson (1973) described a theoretical model of the development of an inversion-capped unstable boundary layer, which implies

$$H(h, t) = -AH(0, t), \tag{1.1}$$

where A is an entrainment parameter varying between 0 and 1. Comparing his theory with the O'Neill data (Lettau and Davidson, 1957), he showed that A seems to fall between 0 and 0.5.

A different approach can be obtained by invoking a similarity assumption for the shape of the temperature profile, in assuming that the temperature deviation $\overline{\Delta T}(t)$ from the stable initial profile is described by a law of the form $\overline{\Delta T} \sim h$ (Figure 1). This latter model corresponds to the approximation assumed by Plate (1971) for the distribution of potential temperature:

$$\bar{\theta}(t) = \bar{\theta}_0 + \alpha h(t) \tag{1.2}$$

where $\bar{\theta}_0$ is the initial potential temperature at the bottom of the fluid and α is a proportionality constant as yet unknown. In the case of zero entrainment, this constant becomes equal to γ. With entrainment, α is less than γ (Figure 2).

This paper describes the time-dependent behaviour of the height $h(t)$ and temperature $\bar{T}(t)$ of the mixed layer and identifies the quantities which determine these values. They can be determined from the fluid properties, the initial temperature gradient γ, and the heat flux $H(0, t)$, all of which affect the entrainment process at the interface between the mixed and stable layers.

The experiment was performed in the laboratory in a glass tank, which was filled with initially linearly thermally-stratified water. The tank was heated from below and the developing mixed layer visualised using shadowgraphs. The initial temperature gradient γ, the bottom heat flux $H(0, t)$, the height of the mixed layer $h(t)$ and vertical temperature profiles $T(z, t)$ were simultaneously measured.

Laboratory experiments were performed in order to test the different closure assumptions mentioned above and to provide a data base for the calculation of the values of A or α. Twenty-two experiments were performed over the range of 0.29 to 0.89 °C cm^{-1} for the initial temperature gradient γ and 0.16 to 1.36 W cm^{-2} for the initial heat flux at the bottom surface.

The initial results have been reported at the Euromech Kolloquium 51 (see: Linden and Turner, 1975). Similar laboratory experiments have been described earlier by Deardorff *et al.* (1969) and by Willis and Deardorff (1974). Nevertheless, there exist some differences in the measuring techniques and the evaluation of the experimental data.

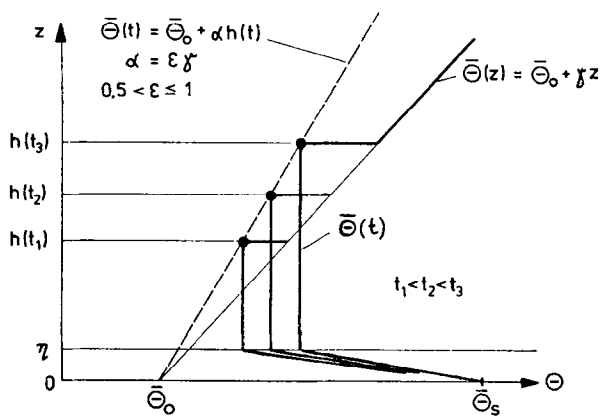

Fig. 2. Geometrical description of Plate's closure equation $\bar{\theta}(t) = \bar{\theta}_0 + \alpha h(t)$ (1.2) for the development of temperature profiles.

2. Theoretical Considerations

The theoretical treatment presented here begins with the same basic equations as used by Plate (1971), Betts (1973), Tennekes (1973), Carson (1973) and Stull (1973). Special attention is given to Plate's closure Equation (1.2).

The equations apply to the case of the atmosphere, i.e., temperatures $\bar{T}$ presented in Figure 1 are replaced by the corresponding potential temperatures $\bar{\theta}$. The bars indicate horizontal averages.

The conservation of energy equation at elevation z at any time t is:

$$\rho c_p \frac{\mathrm{d}\bar{\theta}(z,t)}{\mathrm{d}t} = -\frac{\partial}{\partial z} H(z,t), \tag{2.1}$$

where ρ and c_p are the density and specific heat at constant pressure, $\bar{\theta}(z,t)$ and $H(z,t)$ are the potential temperature and heat flux, respectively (horizontal means). The partial differential Equation (2.1) for $H(z,t)$ can be integrated over z' if $\mathrm{d}\theta/\mathrm{d}t$ is independent of z. This is valid within the limits $\eta \leq z \leq h(t)$ according to the assumption of a spatially constant temperature $\bar{\theta}(z,t)$ inside the mixed layer at any time t. η is the height of the unstable layer and is assumed to be constant. The time origin $t=0$ is given as the beginning of the heating phase, when the stable stratification can be described as $\bar{\theta}(z) = \bar{\theta}_0 + \gamma z$. This implies that the assumption concerning $\bar{\theta}(t)$ is valid only after a critical time t_c, where $h(t) > \eta$ and $t > t_c$. Integration of Equation (2.1) from η to z then leads to a linear decrease of heat flux with elevation z:

$$H(z,t) = H(\eta,t) + \eta\rho c_p \frac{\mathrm{d}\bar{\theta}(t)}{\mathrm{d}t} - \rho c_p \frac{\mathrm{d}\bar{\theta}(t)}{\mathrm{d}t} z. \tag{2.2}$$

This property of the heat flux has been confirmed by the field measurements of Telford and Warner (1964) as well as by the laboratory measurements of Deardorff *et al.* (1969). Writing Equation (2.2) at the inversion height $h(t)$ gives:

$$H(h,t) = H(\eta,t) + \eta\rho c_p \frac{\mathrm{d}\bar{\theta}(t)}{\mathrm{d}t} - \rho c_p \frac{\mathrm{d}\bar{\theta}(t)}{\mathrm{d}t} h. \tag{2.3}$$

$H(h,t)$ may have a negative value as discussed in the introduction of this paper.

If the height of the unstable layer, η, is assumed to be small, the first two terms of Equation (2.3) can be replaced by the heat flux $H(0,t)$ at the bottom of the fluid. Nevertheless, these two terms are taken into account so that the influence of η on the results remains quantifiable. The temperature profile between the constant bottom temperature $\bar{\theta}_s$ and the temperature of the mixed layer $\bar{\theta}(t)$ is assumed to be linear (Figure 1). Therefore, the heat balance at any time t is:

$$\int_0^t H(0,t')\,\mathrm{d}t' - \int_0^t H(\eta,t')\,\mathrm{d}t' = \rho c_p \eta \frac{\bar{\theta}(t) - (\bar{\theta}_0 + \gamma\eta) + \bar{\theta}_s - \bar{\theta}_0}{2}.$$

Differentiation with respect to time t gives:

$$H(\eta,t) + \rho c_p \eta \frac{\mathrm{d}\bar{\theta}(t)}{\mathrm{d}t} = H(0,t) + \frac{\rho c_p \eta}{2} \frac{\mathrm{d}\bar{\theta}(t)}{\mathrm{d}t}. \tag{2.4}$$

A second way of theoretically representing the heat flux $H(h,t)$ is obtained from an

idealisation of the time-dependent temperature profile $\bar{\theta}(z, t)$. Figure 1 illustrates the assumed form of the temperature profile, in which a temperature discontinuity $\Delta\bar{\theta}(t) = \bar{\theta}_0 + \gamma h(t) - \bar{\theta}(t)$ exists at $z = h(t)$.

This discontinuity implies a negative heat flux towards the mixed layer:

$$H(h, t) = -\rho c_p \frac{\mathrm{d}h}{\mathrm{d}t}[\bar{\theta}_0 + \gamma h - \bar{\theta}(t)]\,. \tag{2.5}$$

Equations (2.3) to (2.5) can be combined, resulting in two equations for the three unknown functions $h(t)$, $\bar{\theta}(t)$ and $H(h, t)$. Therefore, a third closure equation is needed. If as closure the well-known relationship:

$$H(h, t) = \rho c_p \overline{(w\theta)}\Big|_h - \lambda \frac{\partial\bar{\theta}}{\partial z}\Big|_h \tag{2.6}$$

is introduced, where w is the vertical velocity and λ is the thermal conductivity of the fluid, detailed information about $\theta(x, y, h, t)$ and $w(x, y, h, t)$ would be necessary. In addition, the problem of the determination of $h(t)$, $\bar{\theta}(t)$ and $H(h, t)$ would be coupled with the solution of the general equations of free convection. This method would be very difficult and would exclude analytical solutions. Therefore, it is preferred to set up a heuristic method of closure, which makes use of empirical constants to be experimentally determined.

Since $\bar{\theta}_0$ is a constant ($\mathrm{d}\bar{\theta}_0/\mathrm{d}t = 0$), elimination of $H(h, t)$ in Equations (2.3) to (2.5) yields:

$$\frac{H(0, t)}{\rho c_p} = \frac{\mathrm{d}}{\mathrm{d}t}[h(\bar{\theta} - \bar{\theta}_0)] - \eta\frac{\mathrm{d}(\bar{\theta} - \bar{\theta}_0)}{\mathrm{d}t} - \frac{\gamma}{2}\frac{\mathrm{d}h^2}{\mathrm{d}t}\,. \tag{2.7}$$

Equation (2.7) contains two unknowns $h(t)$ and $\bar{\theta}(t)$, where the surface heat flux $H(0, t)$ as well as $\bar{\theta}_0$, γ and η are assumed to be known.

Plate's closure Equation (1.2): $\bar{\theta}(t) = \bar{\theta}_0 + \alpha h(t)$ introduces an unknown positive constant α, and postulates as a first-order approximation a linear relationship between $\bar{\theta}(t)$ and $h(t)$. This relationship is justified by the marginal case of zero entrainment, where $\bar{\theta}(t) = \theta_0 + \gamma h(t)$ with $\alpha = \gamma$. Elsewhere, the temperature $\bar{\theta}(t)$ increases with increasing $h(t)$ for $\alpha \leqslant \gamma$. The geometrical representation of Equation (1.2) showing the development of the temperature profiles is illustrated in Figure 2. Henceforth, the parameter will be presented in a dimensionless way by introducing:

$$\varepsilon = \alpha/\gamma\,. \tag{2.8}$$

From Equations (1.2), (2.7) and (2.8), it follows that:

$$\frac{2H(0, t)}{\rho c_p \gamma} = [2(2\varepsilon - 1)h(t) - \eta\varepsilon]\frac{\mathrm{d}h}{\mathrm{d}t} = (2\varepsilon - 1)\frac{\mathrm{d}h^2}{\mathrm{d}t} - \eta\varepsilon\frac{\mathrm{d}h}{\mathrm{d}t}\,. \tag{2.9}$$

Since $\alpha \leqslant \gamma$ and since the last term in Equation (2.9) can be neglected as a first approximation, it follows that ε must lie between 0.5 and 1. Equation (2.9) is a nonlinear differential equation for $h(t)$, and can be integrated over time. Two

alternatives are discussed: with and without inclusion of η, the height of the unstable layer. Omission of η implies $\eta\varepsilon \ll 2(2\varepsilon - 1)h(t)$, a condition which can be shown to be correct. With $\eta \leq 0.5$ cm, $h(t) \geq 10$ cm and $\varepsilon = 0.87$, it follows that the omission of the height of the unstable layer results in an error of less than 3%. Setting $\eta = 0$ and integrating Equation (2.9) over time yields:

$$(2\varepsilon - 1)h^2(t) = \frac{2E(t)}{\rho c_p \gamma}, \tag{2.10}$$

where

$$E(t) = \int_0^t H(0, t')\,\mathrm{d}t'. \tag{2.11}$$

$E(t)$ is the heat transfer from the ground to the atmosphere within the time interval t.

Consideration of the height of the unstable layer, η, implies that Equation (2.9) cannot be integrated from $t' = 0$, because the equation is valid only after a critical time $t > t_c$. Therefore, the integration leads to:

$$(2\varepsilon - 1)h^2(t) - \eta\varepsilon h(t) + \text{const.} = \frac{2E(t)}{\rho c_p \gamma}, \tag{2.12}$$

where the constant cannot be determined theoretically because the values of t_c and η are unknown.

The most striking difference between the equations with and without inclusion of the height of the unstable layer is found by comparing Equations (2.10) and (2.12). Equation (2.10) postulates a quadratic dependence between the heat transfer $E(t)$ and the height $h(t)$ of the inversion layer, whereas Equation (2.10) describes a general parabolic dependence. Equation (2.10) includes only one empirical parameter ε, which is introduced by using Equation (2.8) or (1.2). This parameter can be determined from a linear regression of the experimental results of $E(t)$ and $h^2(t)$. On the other hand, Equation (2.12) involves three unknown parameters ε, η and a constant. Basically these parameters can also be determined experimentally by a least-square method, which correlates $E(t)$ and $h(t)$. Nevertheless, the evaluation of the experimental results has been performed by using Equation (2.10), which has, in addition to simplicity, the advantage of being directly comparable with the results of Carson (1973).

The rise of the inversion height $h(t)$ is given by Equation (2.10). Equations (1.2) and (2.8) define the temperature $\bar{\theta}(t)$:

$$\bar{\theta}(t) = \bar{\theta}_0 + \varepsilon\gamma h(t). \tag{2.13}$$

Equations (2.5), (2.10) and (2.13) can be combined to determine the heat flux at elevation $z = h(t)$:

$$H(h, t) = -\frac{1-\varepsilon}{2\varepsilon - 1} H(0, t) = -AH(0, t). \tag{2.14}$$

This result shows that $H(h, t)$ is directed towards the mixed layer and is a fraction A of the surface heat flux $H(0, t)$, where

$$A = \frac{1-\varepsilon}{2\varepsilon - 1}. \tag{2.15}$$

Equations (2.14) and (2.15) agree with Carson's hypothesis (1.1). Therefore, it can be concluded that the closure Equations (1.1) and (1.2) are equivalent. For this reason, the parameter A can be determined from the experimentally evaluated value of ε, and vice versa.

3. Experimental Equipment and Procedure

The main objective of the experimental work was the simulation of a free convection process beneath stably stratified water within a tank, by means of heating from below. The experiments enabled the testing of assumptions concerning the temperature profiles described already as well as comparison of the measured and theoretical values for $h(t)$ and $\bar{\theta}(t)$. From this comparison, the empirical parameters ε and A could be determined using Equations (2.10) and (2.15).

The experiments were performed in a glass tank, 50 cm wide, 40 cm high and 10 cm deep (Figure 3). A stable stratification was established by allowing water to flow slowly into the tank with constantly increasing temperature. Inside the tank a thermocouple rake permitted measurements of the resulting vertical temperature gradient γ and the floor temperature $\bar{\theta}_0$. At the bottom of the tank, a warm water heat exchanger, capable of producing a constant temperature T_H, was placed. The increase in height $h(t)$ of the mixing layer was perceived using shadowgraphs (Figure 4) and its horizontally averaged values were evaluated from pictures (Figures 5 and 6).

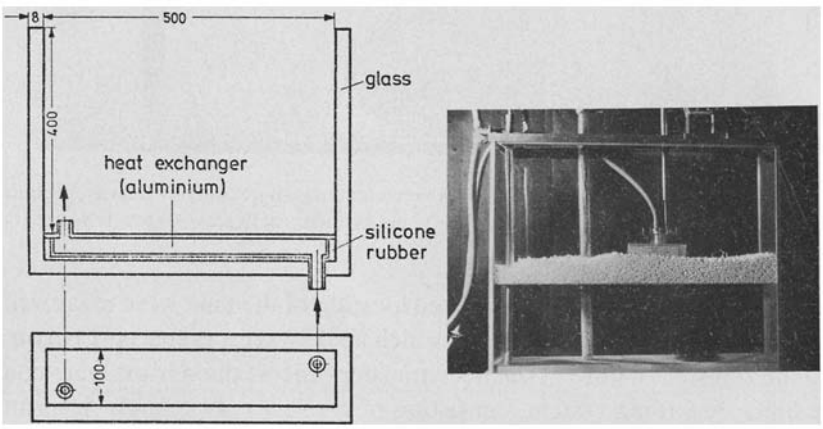

Fig. 3. Elevation and plan views of the experimental tank and heat exchanger. (Dimensions in mm.) The photograph shows the tank during filling operation. The white layer consists of styrofoam spheres, onto which water of constantly increasing temperature is allowed to flow.

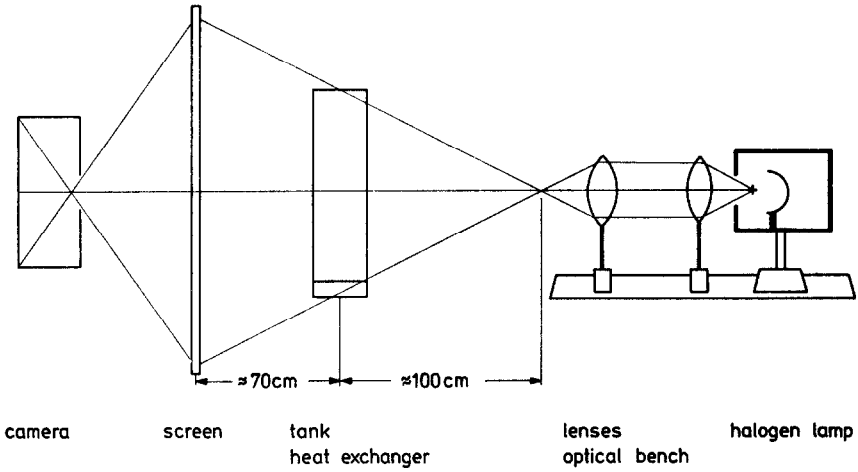

Fig. 4. Components of the visualisation technique.

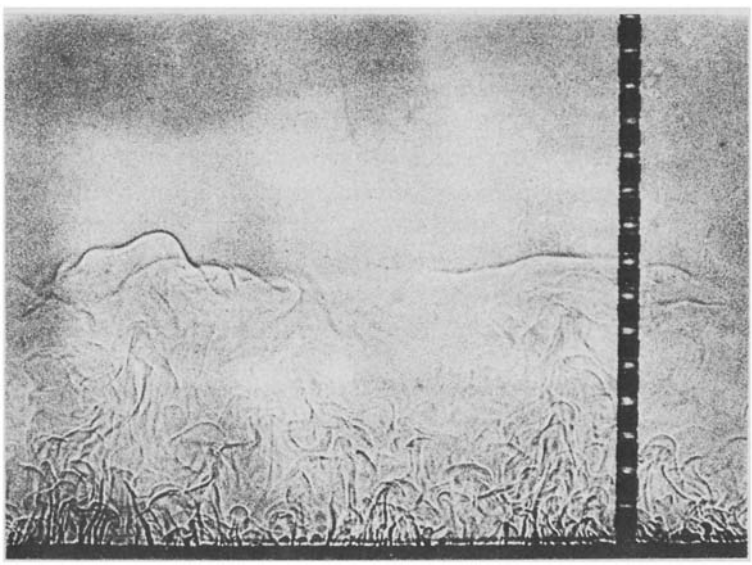

Fig. 5. Shadowgraph of the convection layer, which is identified by 'Schlieren' activity, produced by the simultaneous rise of several thermals. The upper boundary of this layer is nearly horizontal.

Vertical temperature profiles in a fixed location of the tank were measured by the above-mentioned thermocouple rake, which held 31 sensors spaced 1 cm on centre. Due to the transient nature of the heat-transfer process the sensors were connected with a quick recording system, consisting of a selector switch, clock, printer and XY-recorder. Measurement of a temperature profile needed approximaely 45 s. Therefore a numerical procedure was provided for correcting the measured profile to get a simultaneous profile.

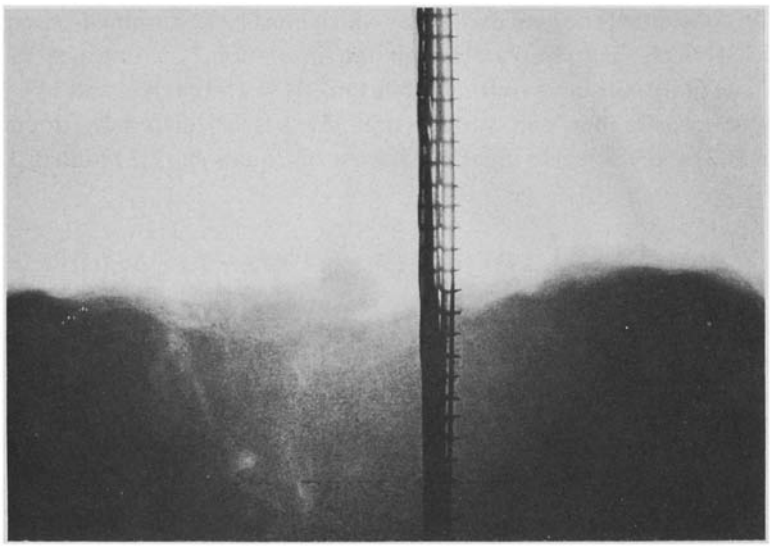

Fig. 6. Photograph of a dyed convection layer. The entrainment process at the boundary of the stable layer is demonstrated by means of the light regions within the dark convection zone.

The time-dependent heat flux $H(0, t)$ at the bottom of the tank was determined from the measured values of the flow-rate Q of water through the heat exchanger and the temperature difference $\Delta T(t)$ between the inlet and outlet. Flow-meter measurements of Q showed almost constant values during an experiment. The temperature difference $\Delta T(t)$ was continuously measured by two Fe-Constantan-thermocouples and was recorded on a XT-recorder. $\Delta T(t)$ always exhibited a time dependence similar to that of a decaying exponential function. The evaluation of $H(0, t)$ was performed as follows.

Initially, the temperature difference between the two ends of the heat exchanger was:

$$T(t=0) = T_H - T_W, \tag{3.1}$$

where T_H is the constant temperature of warm water running through the heat exchanger and T_W is the temperature of the heat exchanger before heating. Later, the increasing water temperature of the mixed layer above the heat exchanger diminished the heat flux $H(0, t)$ and therefore the temperature difference $\Delta T(t)$. A detailed analysis given by Heidt (1975) shows that the heat capacity W, volume V and the heat exchanging surface S of the heat exchanger are relevant for the determination of heat flux $H(0, t)$:

$$H(0, t) = \frac{r}{\rho}\left[\rho c Q \Delta T(t) + (W + \rho c V)\frac{\mathrm{d}\Delta T(t)}{\mathrm{d}t}\right], \tag{3.2}$$

where ρ and c are density and specific heat of water, respectively, and r is a

calibration constant of the heat exchanger which must be determined experimentally and which reflects heat losses through the insulation. Calibrations resulted in $r = 0.90$. The other constants were: $S = 500\ \text{cm}^2$, $W = 150\ \text{cal K}^{-1}$ and $V = 335\ \text{cm}^3$.

The heat transfer per unit surface area $E(t)$ is calculated by integration of Equation (3.2) with respect to time; making use of Equations (2.11) and (3.1) yields:

$$E(t) = \frac{r}{\rho}\left[\rho c Q \int_0^t \Delta T(t')\,\mathrm{d}t' - (W + \rho c V)(T_H - T_W - \Delta T(t))\right]. \tag{3.3}$$

The calculation of $E(t)$ involves the time integral of the temperature difference $\Delta T(t)$, which was measured using an A/D-converter and a digital counter with a time base. All of the experiments were performed in such a way that T_W was very close to the bottom temperature $\bar{\theta}_0$ of the stably stratified water ($T_W \approx \bar{\theta}_0 \approx 20\,^\circ\text{C}$).

Determination of $\bar{\theta}_0$, γ, $h(t)$, $\bar{\theta}(z, t)$, $E(t)$ and t was sufficient to give the complete set of variables which are necessary for testing the theoretical results. Twenty-two experiments were performed for various values of the initial temperature gradient γ and the initial temperature gap $T_H - T_W$ of the heat exchanger. The range of values is given in Figure 7.

The evaluation and representation of the measured data were carried out using computer programs developed for the UNIVAC 1108 of the University of

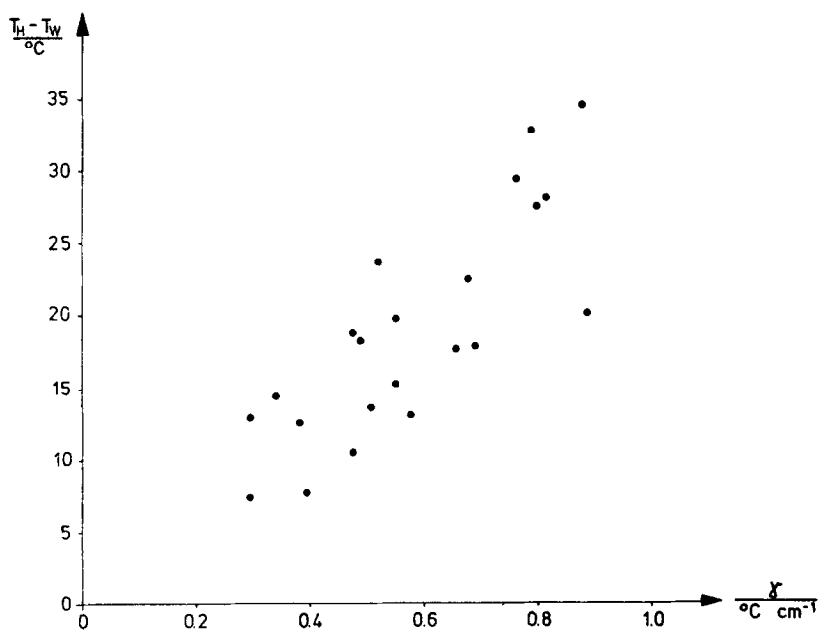

Fig. 7. Summary of the data observed in the experimental program. Each point in the diagram corresponds to the initial conditions of a given experiment.

Karlsruhe. Each experiment included up to 600 input data points, which can be divided into four groups:

(1) experimental constants;
(2) heights of the mixed layer and corresponding time data;
(3) heat transfer data;
(4) temperature profile data.

4. Evaluation and Results

Only sample results of the 22 experiments are shown here. Nevertheless, Table I includes all the data necessary for the verification of Equation (2.10). A more detailed presentation can be found in Heidt (1975).

Figures 8 and 9 show, for three experiments, the heat transfer and the height of the mixed layer as functions of time, respectively. The numbers 7 and 8 refer to two experiments, whose operating conditions were very similar and which can, therefore, be regarded as nearly identical and a test of reproducibility. The time-dependent behaviour of $h(t)$ and $E(t)$ agrees within the error limits of $\pm 3\%$. Comparison with experiment No. 18 shows that increasing the heat transfer $E(t)$ increases $h(t)$, but that the functional correlation between $h(t)$ and $E(t)$ is less than linear.

TABLE I

Listing of the experimental parameters and results

No. –	γ °C×cm^{-1}	$T_H - T_W$ °C	Q cm^3×s^{-1}	a J×cm^{-2}	b J×cm^{-2}	c 10^{-4}×s^{-1}	ε –	R –
1	0.292	12.8	94.8	653.2	632.6	7.69	0.93	0.998
2	0.297	7.3	125.3	280.8	258.2	6.42	0.84	0.992
3	0.340	14.4	75.3	534.9	527.0	10.6	0.90	0.997
4	0.383	12.4	91.3	564.3	534.9	7.62	0.89	0.995
5	0.397	7.6	125.3	173.0	158.7	12.2	0.83	0.994
6	0.475	10.3	106.6	305.2	286.2	11.6	0.88	0.999
7	0.479	18.6	76.1	1073.9	1044.5	7.11	0.91	0.997
8	0.490	18.3	76.1	1022.1	991.1	6.84	0.90	0.998
9	0.508	13.6	93.1	431.6	425.5	9.23	0.84	0.999
10	0.539	23.6	64.3	1130.0	1101.7	7.50	0.85	0.999
11	0.550	19.6	75.5	779.7	737.1	8.30	0.86	0.998
12	0.552	16.2	77.0	453.5	433.0	10.2	0.84	0.999
13	0.574	13.0	94.8	367.6	347.8	11.95	0.87	0.997
14	0.654	16.6	76.1	507.4	468.1	11.2	0.87	0.997
15	0.675	22.4	64.3	1168.6	1140.3	6.64	0.86	0.998
16	0.692	17.8	72.8	612.3	589.5	11.8	0.84	0.995
17	0.766	29.3	55.8	1876.6	1823.7	6.25	0.87	0.999
18	0.789	32.8	64.3	1931.6	1904.1	7.18	0.87	0.998
19	0.796	27.4	54.1	1501.9	1468.3	7.16	0.87	0.998
20	0.815	27.9	54.1	1621.8	1580.1	6.79	0.93	0.999
21	0.877	34.4	47.3	1529.8	1574.0	7.42	0.87	0.998
22	0.887	19.9	69.3	642.2	605.1	10.27	0.79	0.997

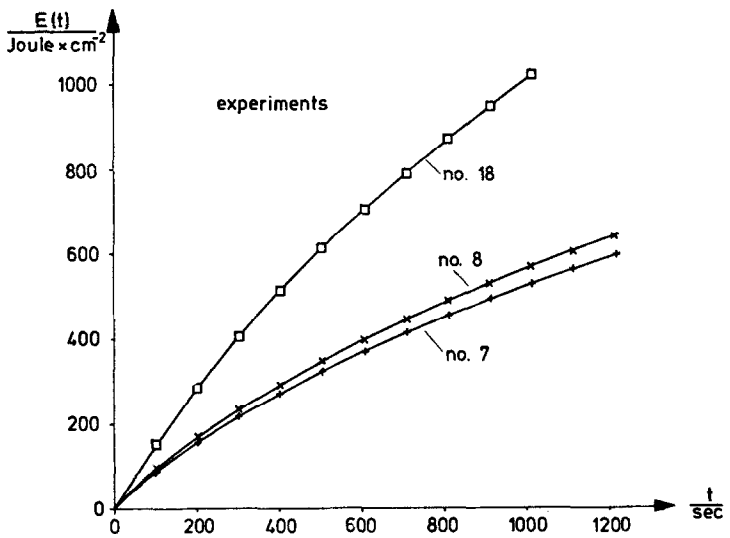

Fig. 8. Time-dependent increase of the heat transfer per unit surface area $E(t)$ according to Equation (3.3) in various experiments. Experiments No. 7 and 8 have approximately the same initial conditions.

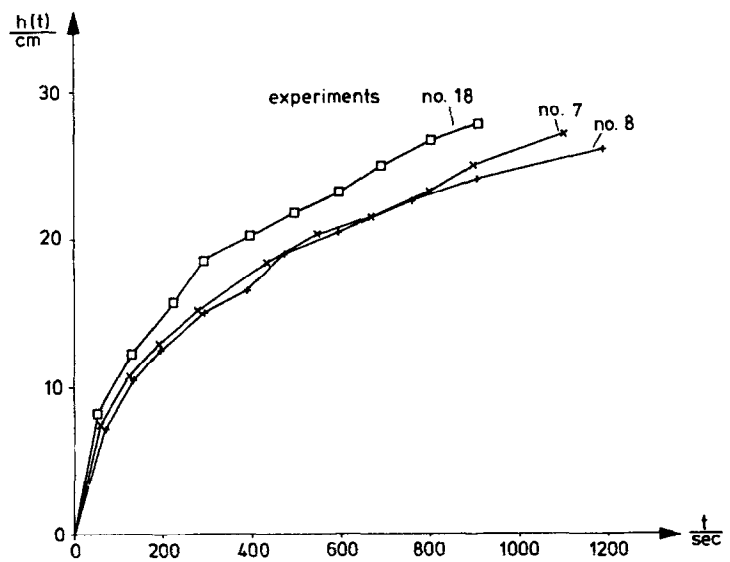

Fig. 9. Time-dependent increase of the convection layer height $h(t)$ in various experiments.

The time-dependent heat transfer function $E(t)$ is determined from measurements using Equation (3.3) at about 12 different times. In all the experiments, however, it was possible to fit these values to an empirical function:

$$E(t) = a - b \exp(-ct), \tag{4.1}$$

where a, b and c are adjustable constants. Neglecting times close to the onset of the

experiment, the deviation of measured from empirically predicted values is less than 0.8%. Therefore, the heat transfer $E(t)$ will be represented by Equation (4.1) whose values can be obtained for the same times as those when the heights of the mixed layer, $h(t)$, were measured.

Figure 10 shows the time-dependent development of temperatures at various elevations measured by the thermocouple rake. At the start of the experiment, temperatures were different at different heights, according to the initial stratification.

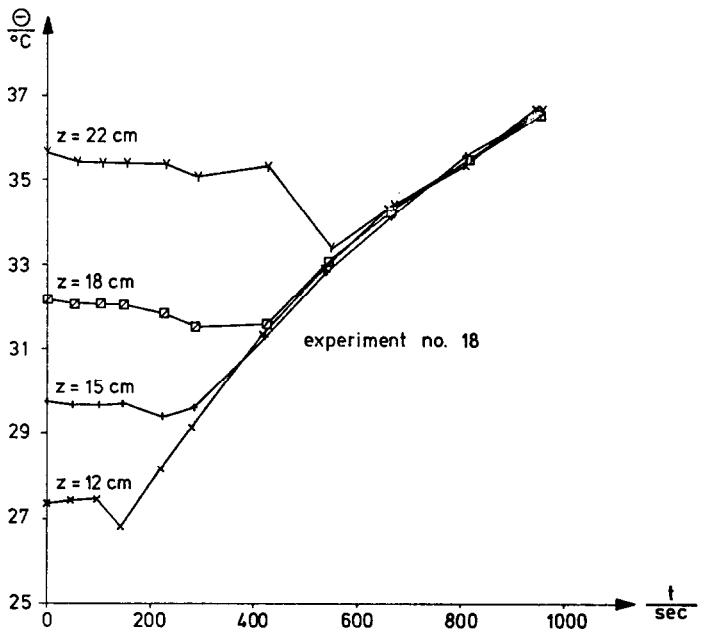

Fig. 10. Time-dependent development of temperatures at selected elevations in experiment No. 18.

At constant elevations, temperatures remained constant or decreased only slightly because of small heat losses to the surroundings. When the convection layer reached these heights, temperatures began to increase. A short time before the arrival of the convection layer a typical temperature decay was generally observed, indicating a net heat flux from the stable layer towards the mixed layer. The increase of temperatures within the mixed layer as well as the increase of height of the mixed layer obey similar time-dependent functions. This is the experimental foundation of the hypothesis for the form of the closure Equation (1.2).

The initial temperature profile for the stable stratification was approximated by a least-square linear regression resulting in values for the floor temperature $\bar{\theta}_0$ and the stable temperature gradient γ. During the heating phase, simultaneous temperature profiles could not be obtained by measurements with the thermocouple rake without corrections due to the finite time difference between the values at the bottom and at the top of the rake. This time difference is known from measurements. Assuming

equidistant time intervals between subsequent profile data, each temperature measurement can be associated with its corresponding time. As the temperature is measured at each elevation for nearly 10 to 15 different times (cf. Figure 10), temperatures at a given time can be calculated by means of linear interpolation.

A typical example of temperature profiles calculated in this way is shown in Figure 11, where the temperature sensors were mounted with a slope towards the bottom of the tank. The slope of the sensor rake avoids falsifying fluid currents which could occur with a vertical rake. Temperatures were found to be homogeneous within the convection layer. Furthermore, it was found that the bottom unstable layer does not protrude upward as far as the lowest sensor, i.e. to a height of nearly 0.5 cm.

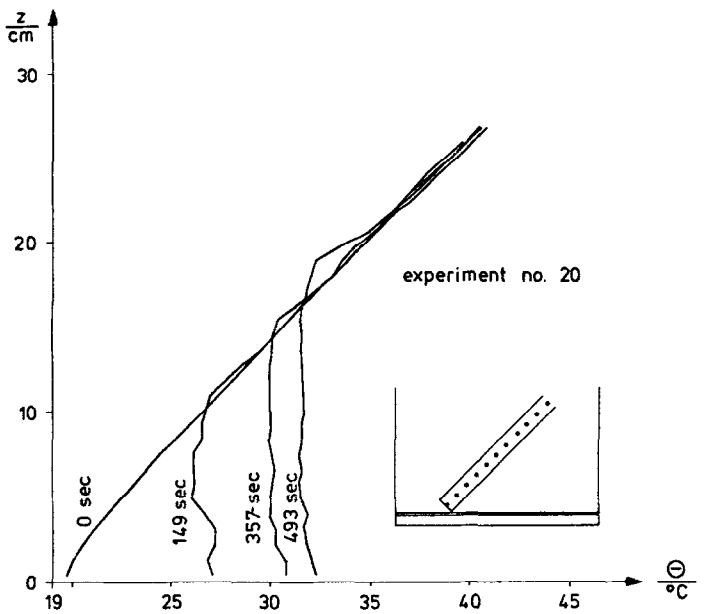

Fig. 11. Time-dependent development of the temperature profiles in experiment No. 20. The temperature sensors were held in a non-vertical orientation. Measurements taken in this manner illustrate the spatial temperature homogeneity in the convection layer.

The shape of the measured temperature profiles justifies the idealisation of temperature profiles presented in Figure 1. The idealised profiles are fitted to the measured profiles in such a way that the sum of areas between the two curves is a minimum. The resulting calculated temperature profiles thus define the height $h_L(t)$ and the temperature $\theta_L(t)$ of the convection layer. The notation L indicates that these values describe local variables, whereas $h(t)$ and $\bar{\theta}(t)$ are horizontally averaged variables. The differences between $h_L(t)$ and $h(t)$ reflect the convolutions of the interface between the mixed layer and the stable layer as illustrated in Figures 5 and 6.

The measurements of the temperature field $\bar{\theta}(z, t)$ can be used to calculate the heat flux $H(z, t)$. Integration of the conservation of heat Equation (2.1) between elevation z and the maximum depth of water, $h_{\max}$, yields:

$$H(z, t) = H(h_{\max}, t) + \rho c \int_{z}^{h_{\max}} \frac{\mathrm{d}\bar{\theta}(z', t)}{\mathrm{d}t} \mathrm{d}z' . \tag{4.2}$$

Since the heat flux at height $h_{\max}$ is only by conduction, it can be omitted, so that

$$H(z, t) = \rho c \int_{z}^{h_{\max}} \frac{\mathrm{d}\bar{\theta}(z', t)}{\mathrm{d}t} \mathrm{d}z' . \tag{4.3}$$

The heat flux $H(z, t)$ can then be determined numerically from measurements by substituting a finite-difference quotient for the derivative of $\bar{\theta}(z, t)$ with respect to time. Typical results are shown in Figure 12, where the linear decrease of heat flux with height was found to be a valid approximation.

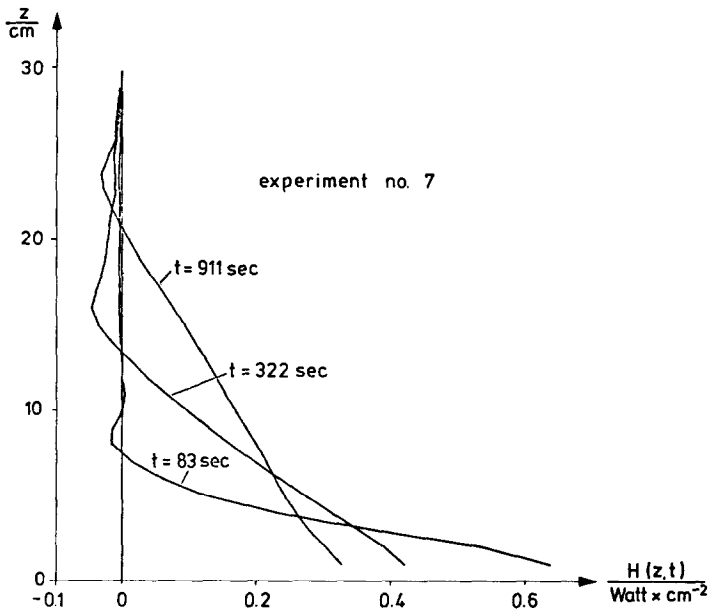

Fig. 12. Time-dependent development of the heat flux profiles according to Equation (4.3) in experiment No. 7.

The experimental confirmation of the assumptions concerning the shape of the temperature profile and the experimentally-determined correlation between $h(t)$ and $\bar{\theta}(t)$ justify the theoretical assumptions presented in Section 2. The validity of Equations (2.10) and (2.13) and the calculation of the values of the parameter ε were also determined from the experimental results.

Equation (2.10) correlates linearly the values of $h^2(t)$ and $E(t)$. Both variables are horizontally averaged. Equation (2.13) includes the temperature $\bar{\theta}(t)$ which is measured only locally.

Figure 13 shows the experimentally-determined linear correlation between $h^2(t)$ and $E(t)$, which is (approximately) in all of the experiments:

$$h^2(t)+\delta = mE(t)\,, \tag{4.4}$$

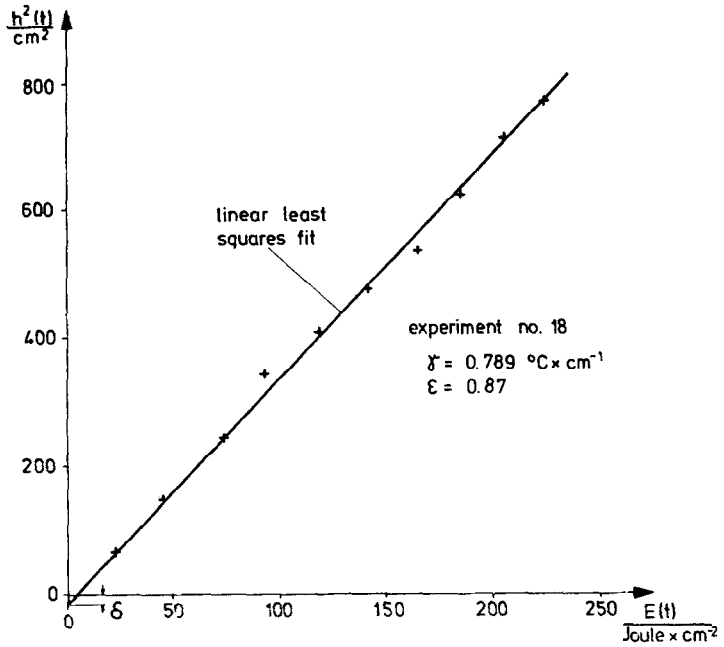

Fig. 13. Experimental relationship between the square of the convection-layer height $h^2(t)$ and the heat transfer per unit surface area $E(t)$. A linear least-square fit of the form $h^2(t) = m \times E(t) - \delta$ approximates the experimental data represented by the points (+). Substitution of $\gamma = 0.789\,^{\circ}\mathrm{C\,cm^{-1}}$ into Equation (4.5) yields $\varepsilon = 0.87$.

where m is the slope and $-\delta$ is the intersection of the h^2-axis at $E = 0$, which normally can be assumed to be zero. Comparing Equations (4.4) and (2.10) and neglecting δ gives:

$$m = \frac{2}{\rho c_p \gamma (2\varepsilon - 1)} \quad \text{or} \quad \varepsilon = \tfrac{1}{2} + \frac{1}{\rho c_p \gamma m}\,. \tag{4.5}$$

This confirms that the dimensionless parameter ε is greater than 0.5 and can be determined from the experimental values of γ and m. The results are listed in Table I, which also contains the correlation coefficients R between $h^2(t)$ and $E(t)$, which test linearity and which were greater than 0.99.

Figure 14 shows the histogram of the measured values of ε which is nearly a constant having a mean value of

$$\varepsilon = 0.87 \tag{4.6}$$

and a total range:

$$0.79 \leq \varepsilon \leq 0.93 . \tag{4.7}$$

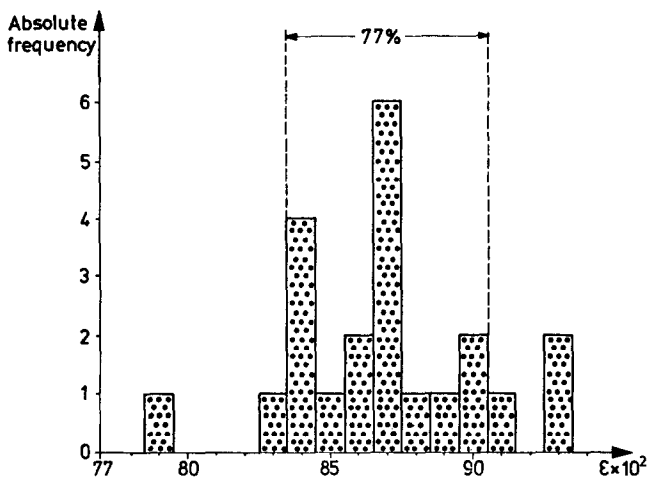

Fig. 14. Histogram of the values of ε determined from all of the experiments.

More than 75% of the experimental results cover the range:

$$0.84 \leq \varepsilon \leq 0.90 . \tag{4.8}$$

Within the calculated values of ε, no systematic dependence on the variables γ, $T_H - T_W$ and Q could be found. Thus, it seems justified to ascribe the scattering of values of ε to the measurement errors associated with the determination of γ and m or $E(t)$ and $h^2(t)$.

The results in Equations (4.6) to (4.8) were introduced into the theory and compared with the laboratory measurements. Figure 15 shows very good agreement between the heights of the mixed layer calculated according to Equation (2.10) and its measured values. The agreement between calculated and measured temperatures of the convection layer is not as good (Figure 16). This is not surprising since horizontally averaged values from theory are compared with temperature values which were measured only locally. In summary, a value of 0.87 for the dimensionless parameter ε and the theoretical relationship given in Equations (2.10) and (2.13) provide a good model for the data measured in the laboratory.

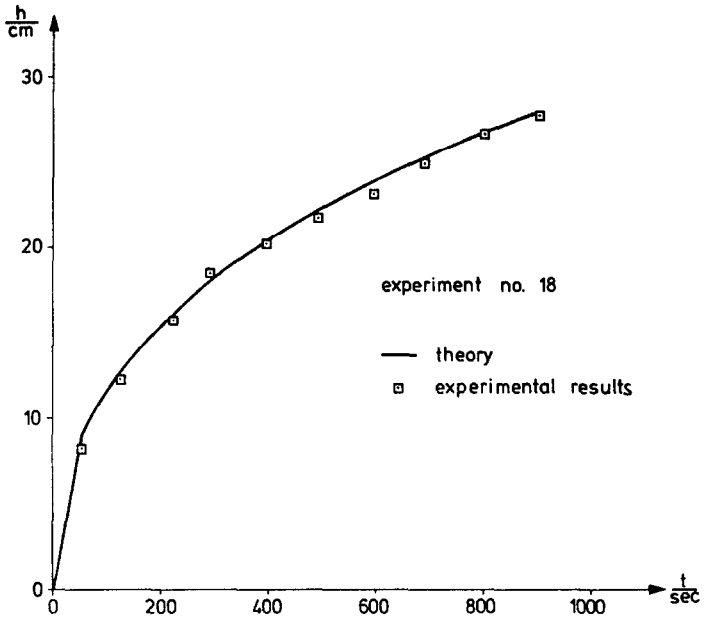

Fig. 15. Comparison of measured and predicted values (Equation (2.10)) of the convection layer height in experiment No. 18.

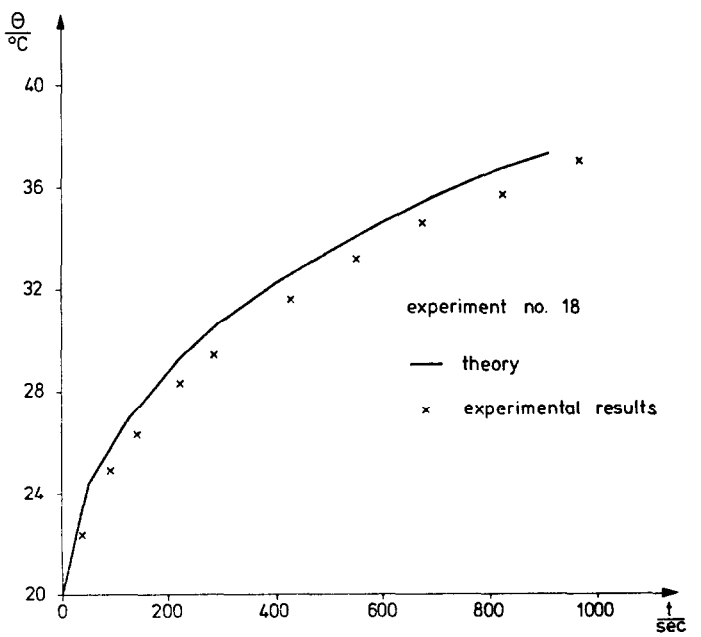

Fig. 16. Comparison of the calculated average convection-layer temperature (Equation (2.13)) and point measurements in experiment No. 18.

5. Applications of the Results and Discussion

A comparison of the results for the parameter ε given in Equations (4.6) to (4.8) with published values can be made only indirectly by calculating the corresponding parameter A from Equation (2.15). Concerning A, various authors assume values which are not very consistent. Nevertheless, some recent values are grouped more closely together. All of the reported results are listed in Table II, including the values of this paper.

TABLE II

Survey of the values of the parameters ε and A as given in the literature including the experimental results of this paper

Author	Year	A	ε
Ball	1960	1	0.67
Lilly	1968	0–1	0.67–1
Betts	1973	0.25	0.83
Carson	1973	0–0.5	0.75–1
Lenschow	1973	0.08	0.93
Tennekes	1973	0.2	0.86
Deardorff	1974	0.14–0.21	0.85–0.89
Heidt	1976		
Mean value		0.18	0.87
Mean value ± one standard deviation		0.12–0.24	0.84–0.90
Total range of the calculated values		0.08–0.36	0.79–0.93

Ball (1960) and Lilly (1968) obtained values of A using a rough simplification of the averaged equation of turbulent kinetic energy. Lilly also considered the case of minimum entrainment $A = 0$ (or $\varepsilon = 1$). Tennekes (1973) took a value of A from meteorological field data (VIMHEX); Carson (1973) from the O'Neill data; and Lenschow (1973) from measurements over the Great Lakes. Deardorff (1974) numerically simulated the data for day 33 of the Wangara experiments and thereby calculated the quotients A of the heat fluxes at the ground and at $z = h$.

Although the values reported in the literature relate to the atmospheric case, whereas the values presented in this paper relate to laboratory experiments in water, there exists satisfactory agreement, especially when only the recently reported values are considered. The mean value of the laboratory experiments is approximately the same as that reported by Tennekes (1973); the interval defined by the mean value ± one standard deviation coincides with the range of values calculated by Deardorff (1974). The value of A stated in Lenschow (1973) is the lowest of the experimental results. The value of the dominant frequency of the experimental results is the same

as the mean value of $\varepsilon = 0.87$ or $A = 0.18$ (Figure 14). The laboratory experiments therefore define more closely the limits of ε or A reported by Carson (1973).

Of course, the use of a model is justified only when the corresponding physical processes are identical or at least similar. For the prediction of the lifting of the inversion layer in the atmosphere or the deepening of the thermocline in a lake, this requirement is partially violated.

In the atmosphere pure windless convection is rather scarce. Usually, wind shear exists, creating mechanical turbulence near the ground. In that case, buoyancy-induced turbulence dominates only at some distance above the ground. In addition, a velocity field often exists in the stable layer, which probably increases shear stresses at the base of the inversion. The influences of humidity and solar radiation may also be important. Furthermore, often a general subsidence of the convective layer is observed, which counteracts the increase of thickness of this layer, making the stable temperature gradient, γ, time dependent (Carson, 1973).

Thermally-stratified lakes or reservoirs are generally affected by fluid currents, which are caused by advection currents, wind, the Earth's rotation or seiches. The effects of wind-shear stress at the water surface produce mechanical turbulence, which leads to the formation of a time-dependent mixed layer. Investigations in this field are described, for example, by Kato and Phillips (1969) and Linden (1975). Furthermore, heat transfer into the water is not a simple boundary condition. Absorption of radiation produces heat sources within the upper layers. Linear temperature profiles beginning at the water surface are therefore rather exceptional.

The various perturbations of the convective process in the atmosphere and in stagnant water are too complex to be investigated in this paper. For testing the applicability of the simple convection model, it would therefore be useful to compare the theoretical results with field data, particularly those which contain an initially linear temperature profile and which include time-dependent values of temperature profiles and heat fluxes. Simultaneous data of this type have been evaluated by Heidt (1976). In all of these cases, the comparisons result in a satisfactory agreement between measured and predicted temperature values.

Only rough calculations using typical values valid for the atmosphere and for lakes have been given in this paper. However, the experimental values are of the same order of magnitude as the theoretical ones.

Warner and Telford (1967) presented atmospheric temperature profiles at various times (Figure 17), from which the heights $h(t)$ and the initial temperature gradient γ can be approximated. While information about the heat transfer $E(t)$ is lacking, it is assumed that the heat flux $H(0, t)$ was sinusoidal, with a time period of 12 h beginning at 07:00 and with a maximum value of 200 W m^{-2} (Priestley, 1959). From Figure 17, γ was found to be approximately 3.7 °C km^{-1}. Calculating $h(t)$ according to Equation (2.10) results in $h = 623$ m at 09:46, 706 m at 10:17 and 845 m at 10:50. The observed values of the cloud base were 557, 700 and 928 m, respectively.

In the case of a lake, substitution of an average temperature gradient $\gamma = 1$ °C m^{-1} and an average heat flux $H(0, t) = 50$ W m^{-2} into Equation (2.10) yields a height of

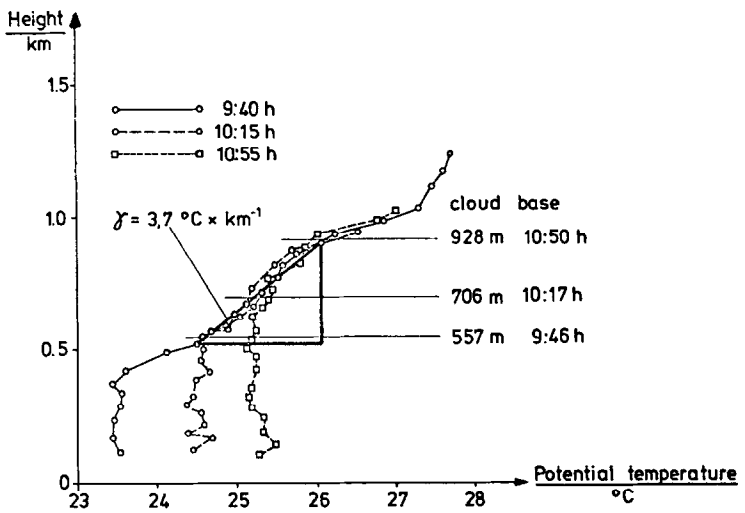

Fig. 17. Field measurements of the time-dependent development of the temperature profiles and the cloud base (after Warner and Telford, 1967).

the epilimnion of 9.2 m after one month. After the second month, the calculated height is 13 m. These values are quite comparable with those observed in nature.

Finally, two points should be mentioned in order to show the limitations and possible refinements of the convection model.

The model is basically a two-layer model assuming homogeneous temperatures $\bar{\theta}(t)$ within the mixed layer and height-dependent temperatures $\bar{\theta}(z) = \bar{\theta}_0 + \gamma z$ within the stable layer above.

The model collapses, if the temperature gradient γ tends to zero, i.e., $h(t)$ becomes infinite according to Equation (2.10). Thus, it is important to determine the smallest allowable gradient γ, for which the model still applies. A possible lower limitation may be given by the reasonable requirement that the Brunt–Väisälä period, $\tau = 2\pi/\sqrt{g\beta\gamma}$, should be significantly smaller than the duration of bottom heating, where g is the gravity constant and β is the thermal expansion coefficient of the fluid.

Another feature of the two-layer convection model is the discontinuity between the temperature of the mixed layer and that of the stable layer. This is a rather strong idealisation of experimentally found temperature profiles. In reality, there exists a finite transition zone within which the temperature gradient changes from infinity to the constant γ. This fact could be modelled, for example, by the addition of a gaussian bell-shaped curve (rotated by 90°) at the top of the mixed layer, joining it to the stable layer in a continuous way. This refinement of the theory has the advantage of better describing the temperature profiles. Furthermore, a diffusion constant D can be derived from the gaussian distribution which can then be used to determine the heat flux at the inversion height. The diffusion constant is of the form

$$D = kV_e h, \tag{5.1}$$

where V_e is the entrainment velocity:

$$V_e = \frac{\mathrm{d}t}{\mathrm{d}h}. \tag{5.2}$$

The factor of proportionality, k, depends on the shape of the temperature profile and has an approximate value:

$$k \approx 0.02. \tag{5.3}$$

Through such a transition zone, it seems possible to combine the studies of the mixed layer with turbulent shear-layer models and to improve the simple profile assumptions for the closure of Equation (2.7).

Acknowledgements

The author is indebted to Prof. E. Plate for many helpful discussions, to Mr F. Heine for his help in the experiments and to Dr M. Markowsky for his help in the English formulation of the manuscript.

The work was supported by a grant of the German Science Foundation (DFG) to the Sonderforschungsbereich 80 at the University of Karlsruhe.

References

Ball, F. K.: 1960, 'Control of Inversion Height by Surface Heating', *Quart. J. Roy. Meteorol. Soc.* **86**, 483–494.

Betts, A. K.: 1973, 'Non-Precipitating Cumulus Convection and its Parameterisation', *Quart. J. Roy. Meteorol. Soc.* **99**, 178–196.

Carson, D. J.: 1973, 'The Development of a Dry Inversion-Capped Convectively Unstable Boundary Layer', *Quart. J. Roy. Meteorol. Soc.* **99**, 450–467.

Deardorff, J. W., Willis, G. E., and Lilly, D. K.: 1969, 'Laboratory Investigation of Non-Steady Penetrative Convection,' *J. Fluid Mech.* **35**, 7–31.

Deardorff, J. W.: 1974, 'Three-Dimensional Numerical Study of the Height and Mean Structure of a Heated Planetary Boundary Layer,' *Boundary-Layer Meteorol.* **7**, 81–106.

Farmer, T. D.: 1975, 'Penetrative Convection in the Absence of Mean Shear,' *Quart. J. Roy. Meteorol. Soc.* **101**, 869–891.

Foster, T. D.: 1965, 'Onset of Convection in a Layer of Fluid Cooled from Above,' *Phys. Fluids* **8**, 1770–1773.

Heidt, F.-D.: 1975, *Zeitlicher Abbau der stabilen Schichtung eines Fluids durch freie Konvektion*, University of Karlsruhe, Ph.D. Thesis.

Heidt, F.-D.: 1976, 'Comparison of Laboratory Experiments on Penetrative Convection with Measurements in Nature,' *Turbulent Buoyant Convection*, International Centre of Heat and Mass Transfer, Dubrovnik, Jugoslavia, pp. 199–210.

Kato, H. and Phillips, O. M.: 1969, 'On the Penetration of a Turbulent Layer into a Stratified Fluid,' *J. Fluid Mech.* **37**, 643–655.

Lenschow, D. H.: 1973, 'Two Examples of Planetary Boundary Layer Modification Over the Great Lakes,' *J. Atmospheric Sci.* **30**, 568–581.

Lettau, H. H. and Davidson, B.: 1957, *Exploring the Atmosphere's First Mile*, Pergamon Press, London.

Lilly, D. K.: 1968, 'Models of Cloud-Topped Mixed Layers Under a Strong Inversion,' *Quart. J. Roy. Meteorol. Soc.* **94**, 292–309.

Linden, P. F.: 1975, 'The Deepening of a Mixed-Layer in a Stratified Fluid,' *J. Fluid Mech.* **71**, 385–405.

Linden, P. F. and Turner, J. S.: 1975, 'Small-Scale Mixing in Stably Stratified Fluids,' *J. Fluid Mech.* **67**, 1–16.

Okubo, A.: 1953, 'A Note on the Growth and Temperature Variation of the Convection Layer,' *Oceanogr. Mag.* **5**, 15–22.

Plate, E. J.: 1971, *Aerodynamic Characteristics of Atmospheric Boundary Layers*, U.S. Atomic Energy Commission, Division of Technical Information, Oak Ridge, Tennessee.

Priestley, C. H. B.: 1959, *Turbulent Transfer in the Lower Atmosphere*, University of Chicago Press, Chicago.

Spangenberg, W. G. and Rowland, W. R.: 1961, 'Convective Circulation in Water Induced by Evaporative Cooling,' *Phys. Fluids* **4**, 743–750.

Stull, R. B.: 1973, 'Inversion Rise Model Based on Penetrative Convection,' *J. Atmospheric Sci.* **30**, 1092–1099.

Telford, J. W. and Warner, J.: 1964, 'Fluxes of Heat and Vapor in the Lower Atmosphere Derived from Aircraft Observations,' *J. Atmospheric Sci.* **21**, 539–548.

Tennekes, H.: 1973, 'A Model for the Dynamics of the Inversion Above a Convective Boundary Layer,' *J. Atmospheric Sci.* **30**, 558–567.

Warner, J. and Telford, J. W.: 1967, 'Convection Below Cloud Base,' *J. Atmospheric Sci.* **24**, 374–382.

Willis, G. E. and Deardorff, J. W.: 1974, 'A Laboratory Model of the Unstable Planetary Boundary Layer,' *J. Atmospheric Sci.* **31**, 1297–1307.